UNDERSTANDING THE SEQUENCE OF DAMAGE IN COMPLEX HYBRID COMPOSITE-METALLIC STRUCTURES SUBJECT TO OUT-OF-PLANE LOADING INVESTIGATED USING COMPUTED TOMOGRAPHY

T. Allen*, S. Ahmed, P.A.S. Reed, I. Sinclair, S.M. Spearing

[1]Faculty of Engineering and the Environment, University of Southampton, United Kingdom
Email: tma1e12@soton.ac.uk

Keywords: Hybrid Structures, Computed Tomography, Quasi-Static Indentation, Low Velocity Impact, Damage Resistance

ABSTRACT

The progression of damage in a hybrid composite-metallic structure subject to out-of-plane loading has been examined throughout an interrupted quasi-static-indentation test using micro-focus computed tomography for damage assessment. Two key damage events were identified from the load-displacement tests. The CT data shows that the first damage mechanisms to occur are yielding of the aluminium substrate and matrix cracking in the CFRP; the onset of these damage mechanisms occurs at a similar point in the loading process. With increasing load, delamination occurred between all plies in the CFRP layer. The bonded interface between the aluminium and CFRP was maintained at lower loads - a crack initiated preferentially within the innermost CFRP ply rather than at the interface between the two materials. The CT data indicates that the second damage event on the load-displacement curve can be attributed to CFRP fibre fracture, consistent with contact forces. This work indicates that relatively low-level out-of-plane loads are likely to cause plastic deformation to the aluminium substrate, whilst the integrity of the fibre in the CFRP is maintained until higher loads.

1 INTRODUCTION

Hybrid composite-metallic structures (HCMS) beneficially combine the characteristics of multiple material systems. HCMS are used in a variety of industrial applications where strength, stiffness and weight are important properties. In service, undesired out-of-plane loading events, such as low velocity impact (LVI), can occur during manual handling and transportation. In order to improve the design for damage tolerance of these structures it is necessary to understand the damage processes when subjected to out-of-plane loading.

The progression of damage mechanisms in composite materials is generally well known [1, 2]. However, the majority of impact research has been focused on plate specimens in order to reduce the effect of the specimen geometry on the response. Alderson and Evans investigated filament wound E-Glass/Epoxy composite tubes under QSI and LVI showing that relatively low loads can cause matrix damage leading to delamination initiation [3]; the study concludes that local crushing was the cause of the first drop on the load-displacement curve. Matemilola and Stronge investigated carbon fibre reinforced pressure vessels with an internal layer of high-density polyethylene [4], concluding that the first load drop was caused by delamination. Curtis *et al.* [5] showed that QSI and LVI are comparable during out-of-plane loading of glass fibre reinforced plastic tubes, however Evans and Alderson showed that this equivalence was dependent on specimen support conditions [6]. The differences highlighted between these studies could be related to differences in the test specimen's material, geometry and layup.

The presence of multiple materials, a non-symmetrical composite layup and a residual stress state makes the response of HCMS complex in comparison to traditional composite plate or tube structures when subject to out-of-plane loading. The nature and sequence of damage mechanisms is not fully understood in HCMS. Many damage mechanisms such as: fibre breaks, delamination, intra-laminar cracks, metallic yield and interface debonding between the different materials may occur. Understanding the order in which these damage mechanisms occur, and the presence of any interdependencies between them will provide valuable insight for damage tolerant design of HCMS. LVI behavior of similar HCMS structures [7-9] has largely focused on the residual mechanical properties after impact events, with little consideration given to the mechanics and progression of damage during loading. The present work aims to improve understanding of the damage process in HCMS in order to better inform the design process for these structures.

2 METHOD AND MATERIALS

2.1 SAMPLE DETAILS

The samples tested in this study were specially manufactured for the purposes of this work. The HCMS investigated was made of a 6061-T6 aluminium alloy shell, carbon fibre reinforced plastic (CFRP) and glass fibre reinforced plastic (GFRP). The thicknesses of the aluminium, CFRP and GFRP were 2mm, 5mm and 1mm respectively. The composite layers were filament wound in a combination of circumferential and wider angle helical warps onto the aluminium shell and cured in an out-of-autoclave process.

2.2 OUT-OF-PLANE LOADING

QSI tests were conducted on a servo-mechanical test machine at a crosshead speed of 2mm/min. The sample was supported with a shallow angle V-groove block to centrally locate the specimen. A 16mm hemispherical indentor was used. Displacement measurement was taken at the crosshead of the machine. In order to account for any flexibility in the test machine a compliance test was completed. The indentor was loaded onto a rigid steel block of similar height to the sample. This was used to calculate a compliance correction that was then applied to all QSI tests to account for the compliance of the load train, and to allow for a better estimate of the responses of the HCMS specimens. The load data in this paper is presented on a scale normalised from the peak load.

2.3 COMPUTED TOMOGRAPHY

The CT scans were completed on a Nikon Metrology HMX μCT scanner at the μ-VIS centre, University of Southampton. A custom jig was used to offset the sample from the centre of rotation to complete a local region-of-interest scan of regions of the sidewall. The scanner has a 225kV X-ray source and Perkin-Elmer 1621 2048 x 2048 pixel flat panel detector. An electron accelerating voltage of 170kV was selected, with a tungsten reflection target and a beam current of 151μA. 3142 projections were taken during the 360º rotation of the sample, with sixteen frames per projection taken to reduce noise. 3D reconstruction with a voxel size of 50μm was created using the filtered-back projection method within the Nikon CT Pro 2.0 package. Image processing and analysis was completed using the software packages ImageJ and VGStudio max 2.1.

2.4 EXPERIMENTAL METHOD

A typical load-displacement curve for the HCMS test specimen reveals two key features of interest (Figure 1). The first is indicative of a reduction in the structural stiffness occurring at ~50% off the top load, the second a distinct load drop at ~95%. To describe the sequence of damage a QSI test was performed, with seven CT scan points along the load path for detailed non-destructive damage assessment (Table 1); the peak load was selected as just after the load drop feature. An interrupted test on a single specimen was used in order to account for potential specimen variability seen in preliminary tests. The specimen was tested ex-situ from the CT scanner; i.e. the scans were completed

in an unloaded condition. After the first scan the sample was loaded to first load step and then rescanned, this was repeated through the remaining load steps.

Scan 1	Scan 2	Scan 3	Scan 4	Scan 5	Scan 6	Scan 7	Scan 8
0 (reference)	0.40	0.45	0.50	0.60	0.75	0.95	1.00

Table 1: CT scanning points

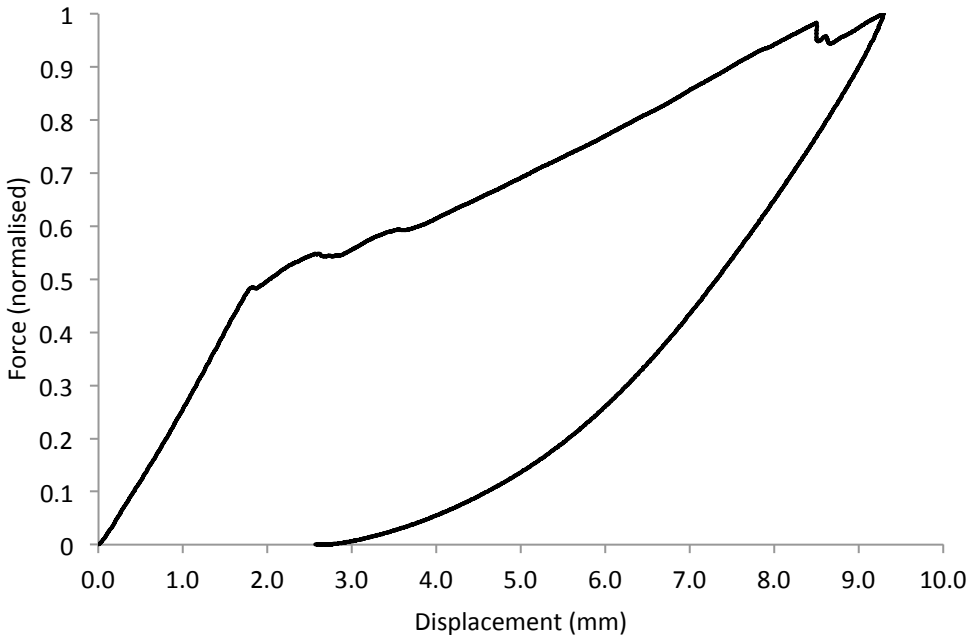

Figure 1: A typical uninterrupted load displacement plot for the HCMS test specimen

3 RESULTS

3.1 QSI LOADING

The interrupted test (Figure 2) followed a very similar profile to the uninterrupted tests (Figure 1) indicating that the use of an interrupted test methodology is sufficient to describe the process of damage in the specimen. The first two load steps at 0.40 and 0.45 demonstrated a largely elastic structural response. After 0.45 the response became non-linear. Between the 0.50 and 0.75 load steps the slope of the load-deflection curve remains approximately constant. Increasing permanent deformation is seen with each load step when the structure was unloaded. At a load of ~0.98 a distinct load drop occurred.

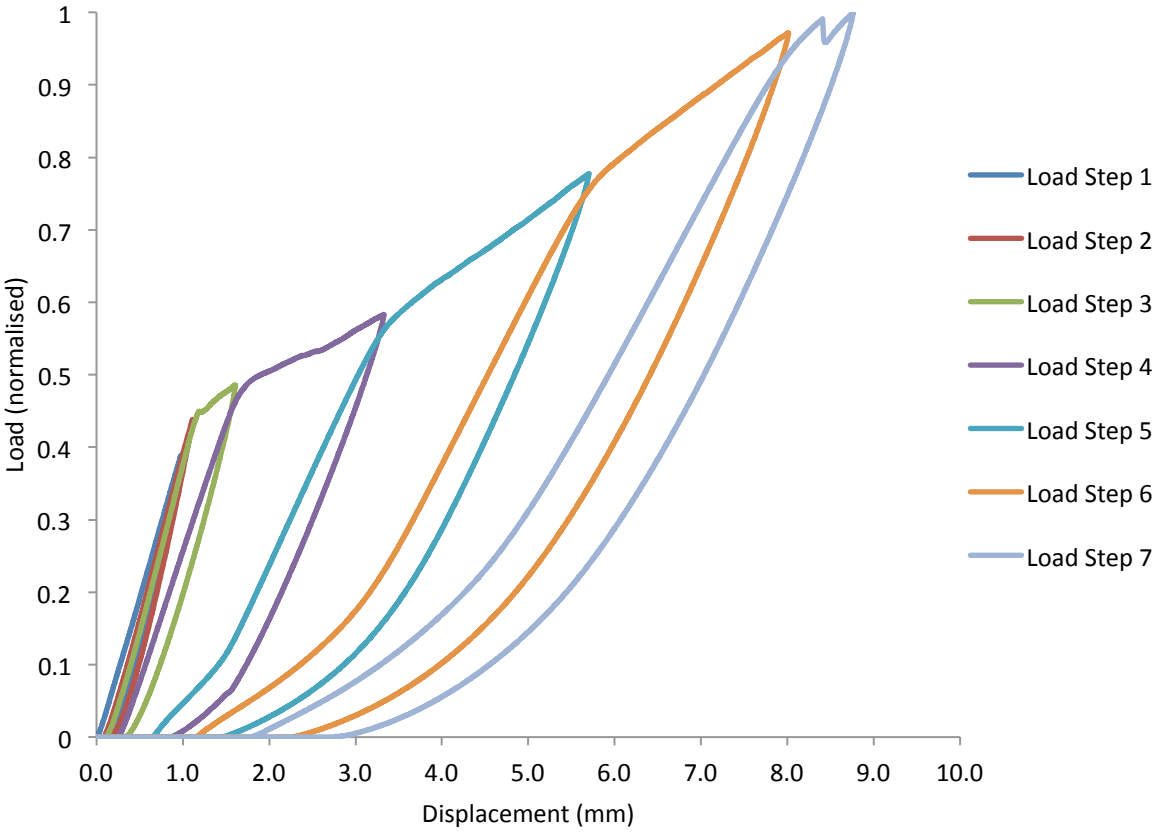

Figure 2: Interrupted quasi-static indentation test

3.2 REFERENCE SCAN

The first scan point was of the sample in the unloaded virgin condition. A cross section in the longitudinal plane shows a typical as manufactured-condition for these HCMS. Due to the out-of-autoclave process a void content of ~3.5% is typical for these structures [10].

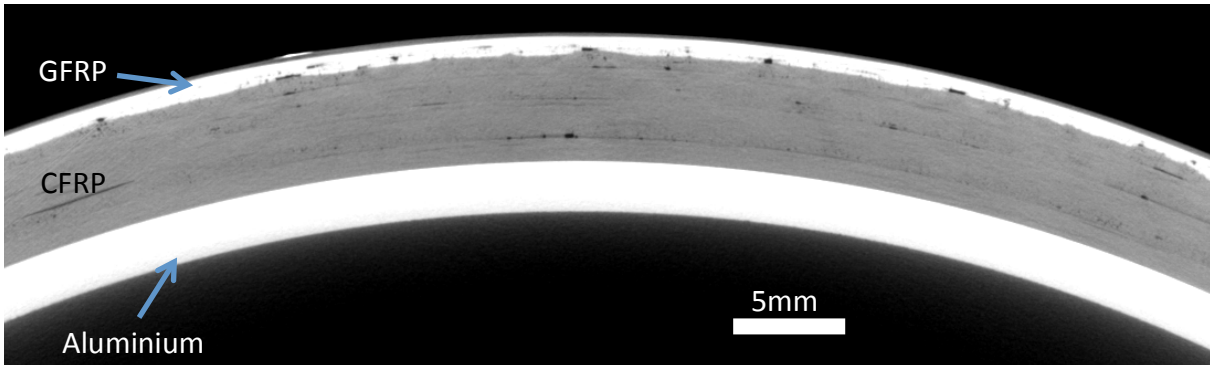

Figure 3: Unloaded reference sample

3.3 PROGRESSION OF DAMAGE

3.3.1 INITIAL ELASTIC RESPONSE

The first load step indicates a largely elastic response (Figure 2), however some permanent indentation was present on the surface of the sample. This was attributed to local indentation in the external gel coat layer and GFRP. No evidence of damage was present in the main structural components of the aluminium and CFRP (Figure 4); this was also the case in the 0.45 load step.

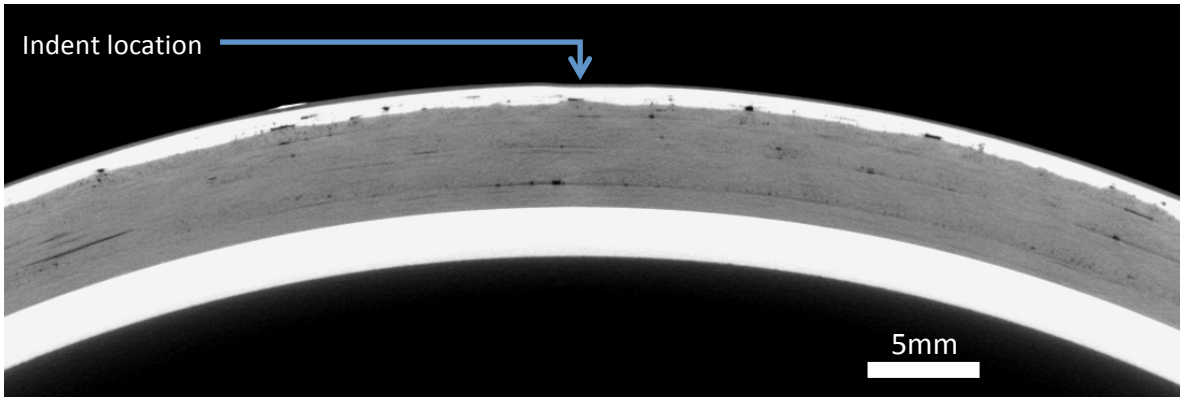

Figure 4: 0.40 load step – centrally located hoop cross section.

3.3.2 DAMAGE INITIATION

When taken to the first load step after the initial structural stiffness change multiple damage mechanisms are present. Plastic deformation of the aluminium substrate and matrix damage to the CFRP and GFRP occurred (Figure 6). The bond between the CFRP and aluminium was maintained at this load step. The residual deformation in the aluminium was measured at 0.2mm (4 voxels) at the indent centre. A "pine tree" damage profile can be seen to be forming with 45 degree shear cracks and the onset of delamination between the innermost and second CFRP ply (Figure 5). There is no evidence of fibre breaks in either the CFRP or GFRP in the scan data. The residual dent on the surface of the specimen can be seen under the indent site in Figure 5, this was clearly visible surface inspection following the loading step.

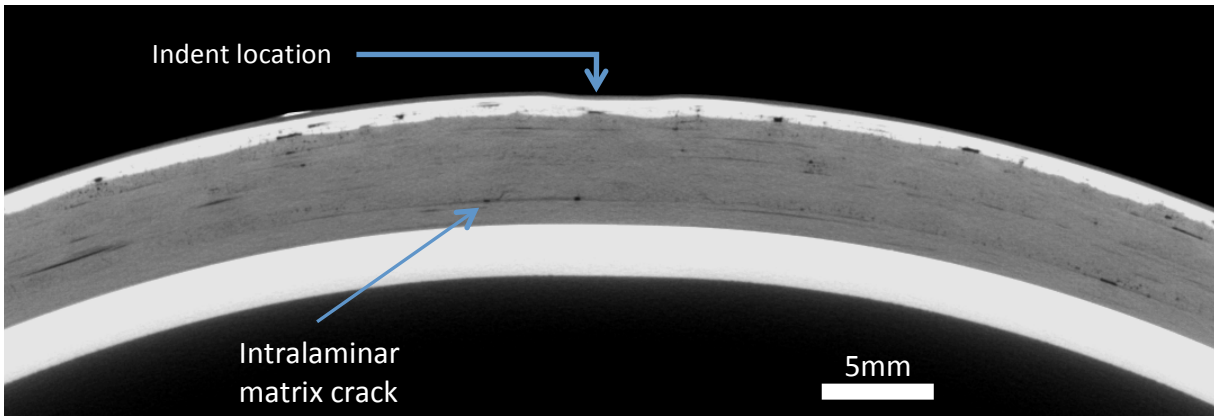

Figure 5: Central cross section at the 0.50 load step

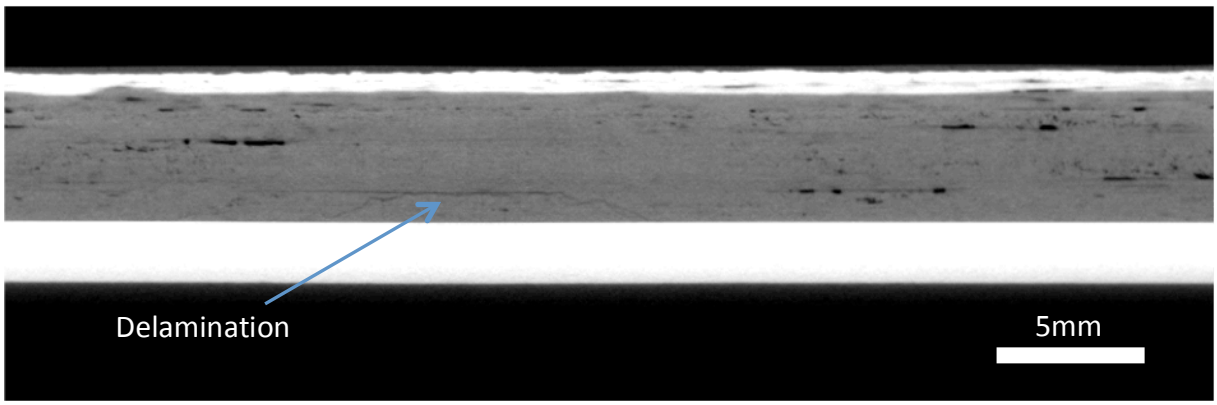

Figure 6: Longitudinal cross section, 5mm from indent centre at the 0.50 load step

3.3.3 PENULTIMATE LOAD STEP

A centrally located slice directly under the indent location is presented in Figure 7. Matrix damage is present throughout all plies in the CFRP, with an undamaged central "cone" directly underneath the indent location, the damage profile (Figure 8) shows broad similarity to CFRP plate impacts [11]. No sign of fibre breaks are present in the CFRP, however directly under the indentor evidence of fibre fracture in the GFRP was present. This was confirmed by looking at a planar slice through the material thickness (Figure 9). Substantial whitening of the GFRP layer was visible from the surface of the specimen and a large residual local indentation.

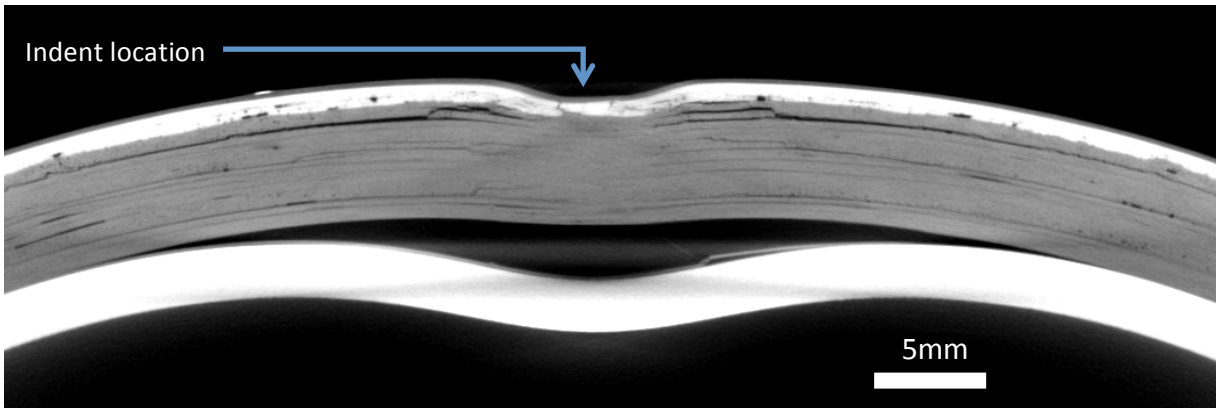

Figure 7: Central hoop cross section after 0.95 load step

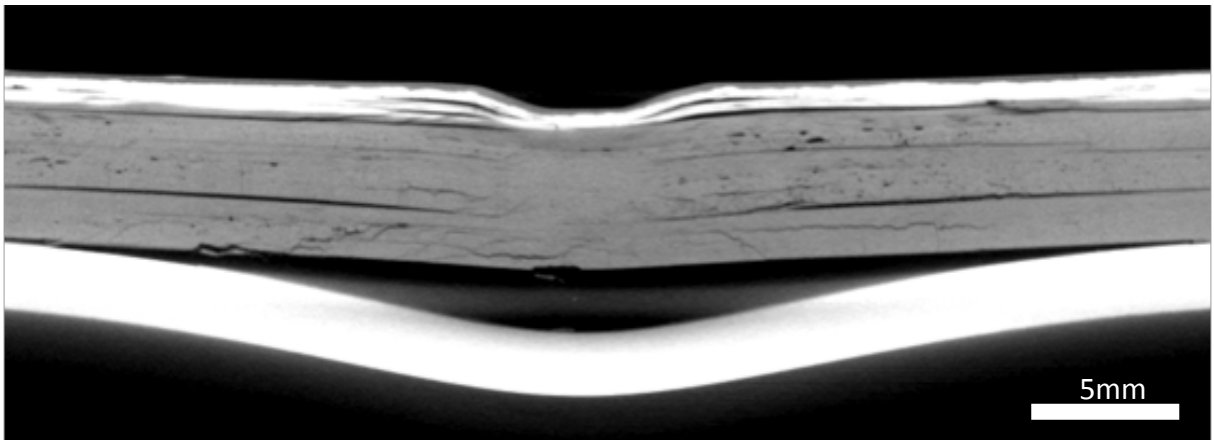

Figure 8: Central longitudinal cross section after 0.95 load step

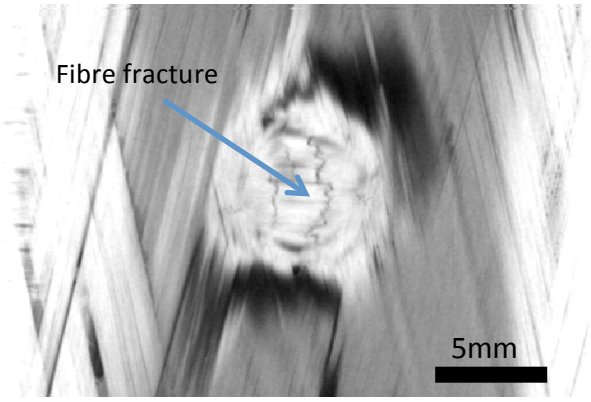

Figure 9: Planar slice at the 0.95 load step showing evidence of GFRP fibre fracture

3.3.4 MAXIMUM LOAD STEP

The purpose of the inspection point at the top load step was to identify the cause of the load drop present in the load-displacement curve. Figure 10 presents a cross-section for comparison with Figure 7 at the previous load step. The CFRP damage shows no sign of progression attributable to the load drop in this plane. In the longitudinal axis of the specimen however the delamination opening at the outermost ply interface in the CFRP increased; highlighted (i) Figure 11. This delamination was present, on both sides of the indentor, in the previous load step in Figure 8 but is distinctly larger at the higher load step. Directly under the tup fibre fracture in the CFRP occurred. This was not present at the previous load step, shown by the comparison between Figure 12A (0.95) and Figure 12B (1.00).

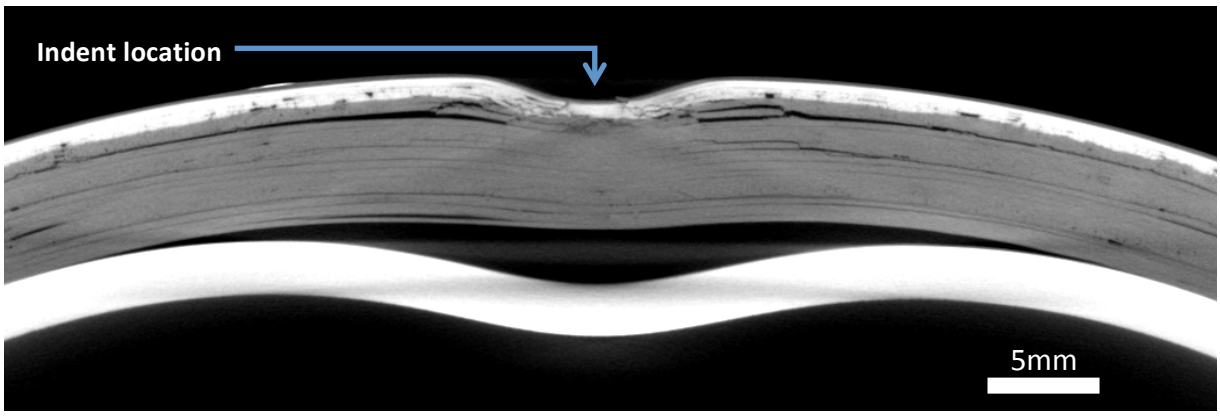

Figure 10: Central hoop cross section at the maximum load step

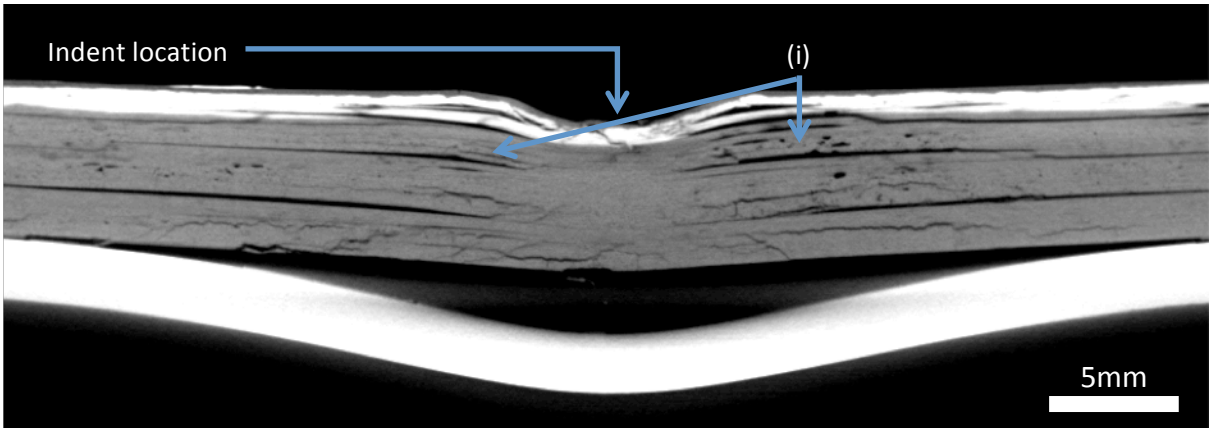

Figure 11: Central longitudinal cross section at the maximum load step

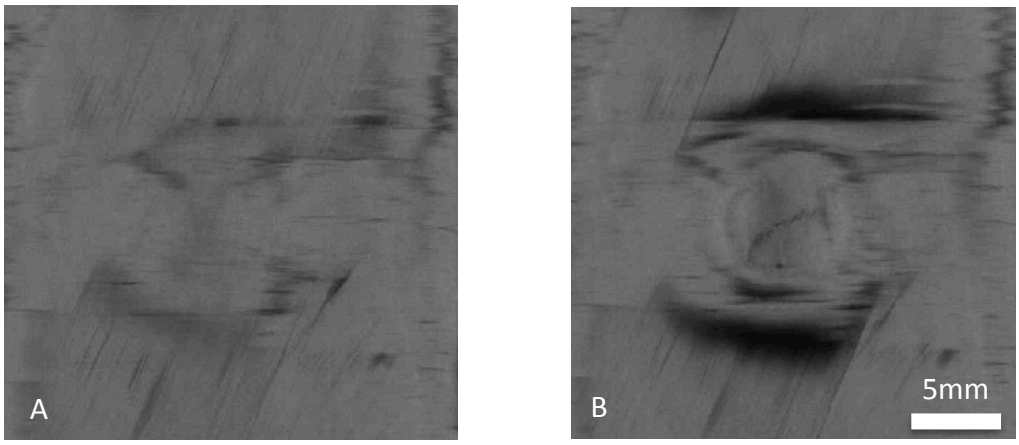

Figure 12: Comparison through material thickness under the indentor in the outer most CFRP ply
A: 0.95 load step; B: Maximum (1.00) load step

4. DISCUSSION

The aim of this study was to describe the progression of damage in HCMS. Two damage events were observed in the load-displacement curve of the specimen (Figure 2). The first event is not a distinct load drop as noted by other authors on purely composite structures [4, 6], but did cause a reduction to the structural stiffness of the test specimen. The scan data from the first inspection point after this event shows that multiple damage mechanism have occurred. Due to the nature of the test it is not possible to conclude which mechanisms occurred first, or if multiple events happened simultaneously. The small amounts of matrix cracking can be expected to have a limited effect on the stiffness of the CFRP [12] and the aluminium is in the location through the thickness of the highest tensile stress under bending. As such, it is proposed that yielding of the aluminium substrate causes the first reduction in the structural stiffness seen on the load-displacement curve. The second feature of interest on the load-displacement curve is a distinct load drop. The CT data confirmed that fibre fracture occurred in the outermost CFRP ply and more severe delamination at the outer most CFRP ply interface between the final two load steps. It is suggested that the fibre fracture can be attributed to this load drop, due to the presence of the delamination in the penultimate load step. The presence of fibre fracture in this location can be expected to reduce the residual tensile strength of the structure [4].

5. CONCLUSIONS

In this study a hybrid composite-metallic structure was subjected to an interrupted quasi-static-indentation test. The data rich methodology, using micro-focus computed tomography for damage assessment, proved successful in describing the damage process, however this limited the scope of the study to a single representative specimen. Two key damage events were identified from the load-displacement curve. These were attributed to yielding of the aluminium substrate and fibre fracture in the CFRP from the evidence in the CT data. This work indicates that relatively small out-of-plane displacements may cause plastic deformation to the aluminium substrate, whilst the integrity of the fibre in the CFRP is maintained until higher load events.

ACKNOWLEDGEMENTS

The authors would like to acknowledge the EPSRC for supporting this work financially. Thanks must also be given to the μ-VIS centre at the University of Southampton for facilitating the CT scanning of this work and to Mr David Beckett for his contribution to the jig manufacture.

REFERENCES

[1] Richardson, M.O.W. and M.J. Wisheart, *Review of low-velocity impact properties of composite materials.* Composites Part A: Applied Science and Manufacturing, 1996. **27**(12): p. 1123-1131.

[2] Reid, S.R., Zhou, G., *Impact Behaviour of Fibre-Reinforced Composite Materials and Structures*. 2000, Cambridge.

[3] Alderson, K.L. and K.E. Evans, *Failure mechanisms during the transverse loading of filament-wound pipes under static and low velocity impact conditions.* Composites, 1992. **23**(3): p. 167-173.

[4] Matemilola, S.A. and W.J. Stronge, *Low-Speed Impact Damage in Filament-Wound CFRP Composite Pressure Vessels.* Journal of Pressure Vessel Technology, 1997. **119**(4): p. 435-443.

[5] Curtis, J., et al., *Damage, deformation and residual burst strength of filament-wound composite tubes subjected to impact or quasi-static indentation.* Composites Part B: Engineering, 2000. **31**(5): p. 419-433.

[6] Evans, K.E. and K.L. Alderson, *Low velocity transverse impact of filament-wound pipes: Part 2. Residual properties and correlations with impact damage.* Composite Structures, 1992. **20**(1): p. 47-52.

[7] Kobayashi, S., *Effect of autofrettage on durability of CFRP composite cylinders subjected to out-of-plane loading.* Composites Part B: Engineering, 2012. **43**(4): p. 1720-1726.

[8] Kobayashi, S. and M. Kawahara, *Effects of stacking thickness on the damage behavior in CFRP composite cylinders subjected to out-of-plane loading*. Composites Part A: Applied Science and Manufacturing, 2012. **43**(1): p. 231-237.

[9] Wakayama, S., et al., *Evaluation of burst strength of FW-FRP composite pipes after impact using pitch-based low-modulus carbon fiber*. Composites Part A: Applied Science and Manufacturing, 2006. **37**(11): p. 2002-2010.

[10] Allen, T., Scott, A. E., Hepples, W., Spearing, S. M., Reed, P. A., Sinclair, I. *Investigating damage resistance of hybrid-composite metallic structures using multi-scale computed tomogrpahy*. in *European Conference on Composite Materials*. 2014. Seville.

[11] Bull, D.J., S.M. Spearing, and I. Sinclair, *Observations of damage development from compression-after-impact experiments using ex situ micro-focus computed tomography*. Composites Science and Technology, 2014. **97**(0): p. 106-114.

[12] Abrate, S., *Impact on Composite Materials*. 1998, New York: Cambridge University Press.